MyCoast model and setup description

The coastal high resolution forecast system WCOOF (Western Channel Observatory Operational Forecast) initially developed through MyCoast Interreg project (EAPA_285/2016, http://www.mycoast-project.org/), is embedded within the CMEMS NorthWestShelf-MFC (Monitoring Forecast Centre) . It provides real-time (daily) short-term two-day hydrodynamic 3D forecast of a range of physical parameters (currents, temperature, salinity and sea-level) and one day hindcast. WCOOF consists of a combination of an ocean model, FVCOM (v4.3, http://fvcom.smast.umassd.edu/fvcom/); and atmospheric model, WRF (v4.0, https://www.mmm.ucar.edu/weather-research-and-forecasting-model); and a local river forecast model all managed through the MetOffice scheduler ROSE (https://metomi.github.io/rose/doc/html/index.html).

The ocean model used is the Finite Volume Coastal Ocean Model (FVCOM), a prognostic, unstructured-grid, finite-volume, free-surface, 3D primitive equation coastal ocean circulation model written in ANSI FORTRAN 95 (Chen, Liu et al. 2003). FVCOM solves the 3D momentum, continuity, temperature, salinity, and density equations by computing fluxes between unstructured triangular elements. Vertical turbulent mixing is modelled with the General Ocean Turbulence Model (GOTM) using a κ-ω formulation (Umlauf and Burchard 2005) whilst horizontal mixing is parameterised through the Smagorinsky scheme (Smagorinsky 1963) with a coefficient of 0.1. The vertical grid in FVCOM is described in terrain following (sigma) coordinates where shallower areas resolve vertical structure with finer detail.

The Western Channel Observatory (WCO) model domain covers the Tamar estuary and nearshore area in the south-west of the UK between longitudes -4.81°E to -3.80°E and latitudes 49.72°N to 50.52°N. It resolves the coastal intertidal areas which are present inside the estuarine area. A minimum depth of 20cm determines the transition between wet and dry areas in intertidal slopes.

The model domain is defined by the initial coastline, derived from the Global Self-consistent, Hierarchical, High-resolution Shoreline (GSHHS, v2.3.7) and sampled at resolutions of 10m (Wessel and Smith 1996). Some aspects such as ports or small coastal indentations have been manually removed from the coastline. The model unstructured grid is constructed with triangles such that the resolution is controlled by the water depth, bathymetry gradient, coastline curvature and coastline resolution using a size function to build spatially varying element sizes to satisfy the hydrodynamic requirements. This approach ensures that areas with complex coastlines and shallow water depths have smaller elements to ensure tidal wave propagation is well resolved (Legrand, Deleersnijder et al. 2007). As such, the grid resolution varies across the domain with a mean triangle length of 144m. Resolution is finest within the estuary area with a minimum side length of 27m. It is coarser outside the estuary and has a maximum at the open boundary of 8.5km. The model uses terrain following sigma coordinates of 24 equidistant levels throughout the domain.

Water depth within the model domain uses the EMODNET bathymetry product with a nominal resolution of 1/16 deg. In the estuary and very nearshore areas (< 20m) the data have been complemented with local data sources of Lidar, single and multi-beam surveys accessed through the

Coastal Channel Observatory (CCO, https://www.channelcoast.org/). The CCO data was re-projected from its original projection (OSGB) to WGS84 and concentrated and averaged into a 20m regular grid using the Generic Mapping Tools (GMT 5.3.2) software (http://gmt.soest.hawaii.edu/). The merged dataset was processed using the ROMS toolbox for bathymetry processing downloaded from https://github.com/dcherian/tools. The scattered bathymetry was interpolated to 25m and smoothed iteratively to achieve a Haney number less than 2 (Haney 1991).

Atmospheric boundary data as heat fluxes and surface stresses are from a locally run Weather Research and Forecasting (WRF) model with a 3 level nested setup and a final resolution of 3 km. WCOOF includes a daily 3-day forecast within ROSE using initial conditions from the Global Forecasting System (GFS).

The open boundary conditions for temperature, salinity, surface elevation and velocities are from the hourly North West Shelf data product, retrieved via the CMEMS service. The hourly currents and surface elevation are pre-processed to remove the tidal signal. The tidal components at the boundaries are then calculated from FVCOM 3D tidal simulations of the same model domain forced by TPXO tidal surface elevation time series input at the open boundary calculated as 10 minute intervals from the TPXO Tidal Model Driver (TMD) MATLAB toolbox (Egbert, Bennett et al. 1994, Egbert and Erofeeva 2002) using the OSU Tidal Inversion Software (OTIS) European regional tidal solution (Egbert, Erofeeva et al. 2010). An initial simulation of 8 months was then analysed over 5 consecutive nodal bands starting from the most exterior boundary using the python implementation of the MATLAB u-tide toolbox ((Codiga 2011) https://github.com/wesleybowman/UTide). The harmonic analysis was then used to predict the tidal variables and imposed at the 5-node wide nesting region. The hourly non-tidal signal from CMEMS service is then linearly added to the tidal solution.

The WCOOF river model provides river flow and temperature inputs to the WCOOF hydrodynamic model for ten single river inputs. River flows are predicted from integrated river catchment precipitation and mean temperature using a dense layer neural network model. The python Keras package is used to implement the neural network and a lagged history of up to a week for temperature and up to a month for precipitation are used as inputs. The networks were trained on 10 years of river flow gauge data from the UK National River Flow Archive. River temperature is predicted using a multiple linear regression model based on mean catchment air temperatures for the past three days. The regression is based on temperature observations from the Environment Agency river monitoring database and includes observation height as a proxy for upriver distance.

Model Validation

The Model has been run with both AMM7 and AMM15 boundary conditions and results have been compared against existing observations (Figure 1) both inside the estuary (Plymouth Sound) and at a coastal location (L4 station). AMM7 simulations include years 2016-2018 while AMM15 forced simulations correspond to 2019-2021.

For the assessment we have combined targeted mooring deployments of ADCP instruments at station L4, routine observations of water column hydrography at stations L4 and E1 (https://www.westernchannelobservatory.org.uk/data.php), underway observations by PML RV Quest on her weekly/bi-weekly visits to L4 and E1, sea surface observations from the seawater sensor packages installed in the L4 and E1 buoys (https://www.westernchannelobservatoryorg.uk/buoys.php) and atmospheric observations from the same buoys and from the recently established Penlee Point Observatory (https://www.westernchannelobservatory.org.uk/penlee/). Since 2018 we have made four Acoustic Doppler Current Profiler (ADCP) deployments at L4 station with different lengths and covering the major oceanographic seasons. In addition, we have collaborated with the University of Plymouth to develop a yearly field campaign with second year's Marine Science students to deploy 3 ADCP moorings in the estuarine area of the model domain (Figure 1).

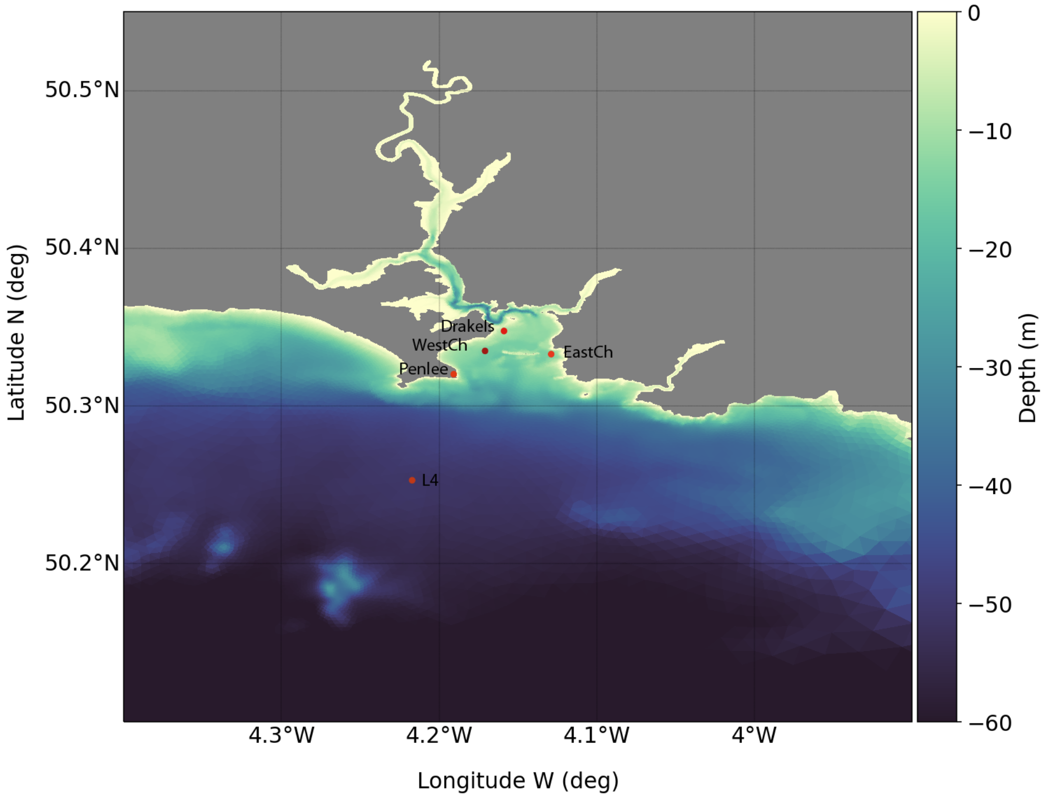

Figure 1 Bathymetry of Model domain and location of stations used for Validation.

Atmospheric model validation

The WRF component of the system has been compared to observations from Penlee coastal observatory and L4 atmospheric package with data available from years 2016 and 2018. The results from linear regressions comparing observations and hourly model ouputs and measures of goodness of fit (Table 1) indicate that offshore conditions (L4) are better reproduced than coastal ones (Penlee) at the finest resolution (3km) of our WRF implementation. This is particularly true of the V wind component, as it is most affected by coastal orography in this region. Wind speed is slightly over estimated offshore (L4, correlation coefficient of 1.15, with r^2 of 0.95) as a result of over estimating the U component (Mean Absolute Error, MAE of 1.47 m s^{-1}). This is less evident near the coast where the fit worsens (wind speed and components r^2 ranges 0.6-0.8 and correlation coefficients 0.98-0.71), over estimation is more dependent on wind direction (e.g. Figure 2), but U component is still better resolved than the V component.

Table 1Summary statistics of model-observation comparisons for the land coastal station Penlee and offshore station L4.

Station	Variable	Year	Correlation	R2	Bias	Root Mean Square	Mean Absolute Error
L4	Wind Speed	2016	1.15	0.95	-1.04	1.82	1.47
L4	Relative Humidity	2016	1.02	0.99	-2.06	6.37	4.86
L4	U wind component	2016	1.08	0.85	-0.26	2.30	1.79
L4	V wind component	2016	0.91	0.62	0.43	2.30	1.77
L4	Air pressure	2016	1.00	1.00	1.92	2.02	1.92
Penlee	Wind Speed	2016	0.99	0.82	-0.99	3.44	2.66
Penlee	Relative Humidity	2016	0.98	0.99	0.35	10.08	7.90
Penlee	U wind component	2016	1.05	0.68	-0.25	3.61	2.79
Penlee	V wind component	2016	0.62	0.37	-0.29	4.23	3.26
Penlee	Air pressure	2016	1.00	1.00	1.39	2.77	1.79

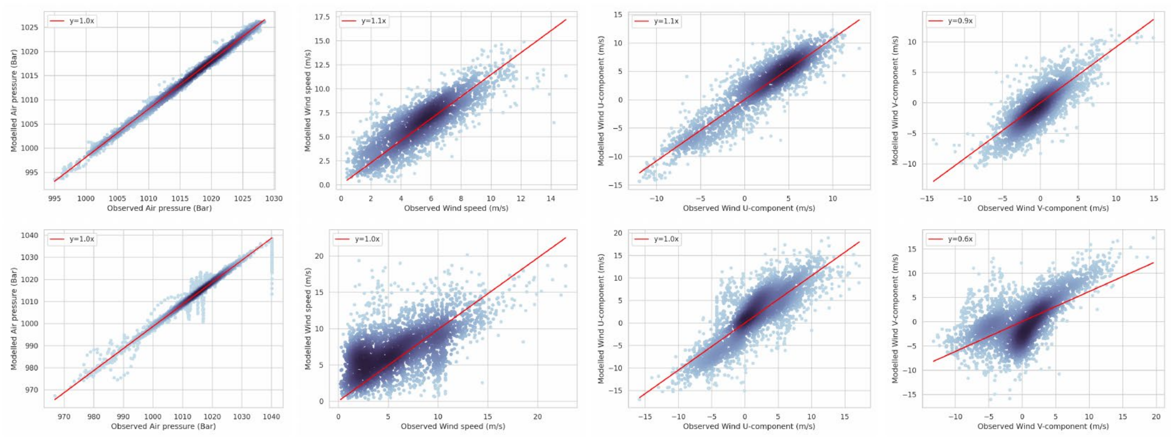

Figure 2 Scatter plot of atmospheric variables at L4 (top) and Penlee (bottom) for [left to right], air pressure, wind speed, u and v wind components.

Hydrodynamic model validation

The model performance has been evaluated against all available data, both inside the estuarine area and in PML's coastal station L4 (Figure 1). The observations represent a wide range of conditions (calm and storm weather, spring and neap tides, high and low riverine inputs). For current measurements, at least two different instruments were used (Table 2). While the model results represent instantaneous hourly values, the observations range from 10 min to 20 min averages. All ADCP data have been processed with only minimal quality controls and so include both tidal and non-tidal processes.

Table 2 Details of ADCP deployments used in the evaluation of the operational model. The deployments encompass five locations: L4, a deep coastal station part of the WCO, three in the Plymouth Sound (Drake's Island, West and East channels, and one in Turnchapel in the Plym estuary.

Station	Instrument	Year	Period	Duration	Season
L4	RDI Workhorse 600	2010	2010-07-28 to 2010-08-11	15 days	Summer/Stratified
L4	RDI Sentinel V50	2018	2018-07-13 to 2018-09-24	73 days	Autumn/Stratified
L4	RDI Sentinel V50	2019-2020	2019-12-05 to 2020-01-20	46 days	Winter/Mixed
L4	RDI Sentinel V50	2020	2020-06-01 to 2020-08-07	66 days	Summer/Stratified
L4	RDI Sentinel V50	2020	2020-09-07 to 2020-11-23	76 days	Autumn/transition
Drake's Island	RDI Workshorse 1200	2017	2017-05-02 to 2017-05-11	8 days	Spring/Stratified
East channel	RDI Workhorse 600	2017	2017-05-02 to 2017-05-11	8 days	Spring/Stratified
West channel	2017	Not Processed	Not Processed	Not Processed	Spring/Stratified
Drake's Island	RDI Workshorse 600	2019	2019-05-07 to 2019-05-16	8 days	Spring/Stratified
East channel	RDI Workhorse 1200	2019	2019-05-07 to 2019-05-16	8 days	Spring/Stratified
West channel	Nortek AWAC	2019	2019-05-07 to 2019-05-16	8 days	Spring/Stratified
Turnchapel	RDI Workshore 600	2020	2020-10-09 to 2020-10-27	17 days	Autumn/Stratified
West channel	RDI Sentinel V50	2021	2021-03-24 to 2021-04-08	15 days	Spring/Stratified

The Plymouth Sound is the estuarine area that was sampled with 3 ADCP moorings on several years (Figure 3). The Plymouth Sound is a restricted embayment that exhibits large spatial variations and sharp gradients in both currents and hydrography as a result of the presence of two estuaries entering on the northwest (Tamar) and northeast (Plym), a narrow deep channel by Devil's Point, Drake's Island and the Breakwater, which constrains ocean-estuary exchanges to two channels, (west and east channels).

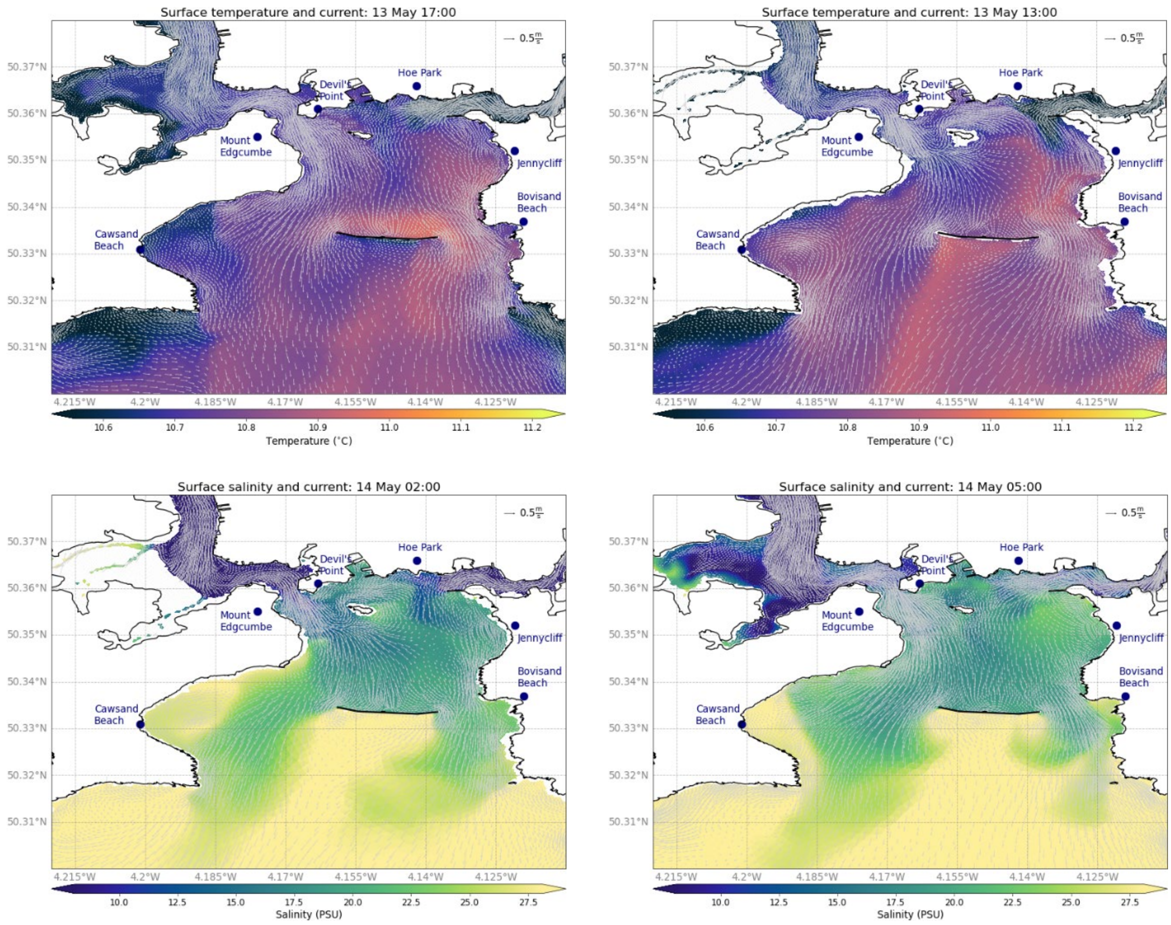

Figure 3 Snapshots of surface currents overlaid on surface temperature (top) and salinity (bottom) during two floods and ebbs. The graphs illustrate the complicated circulation patterns in Plymouth Sound as a results of the confluence of two estuaries (the Tamar and the Plym) and the presence of Drake's Island and the Breakwater. These include shadow regions, jets, fronts and re-circulation cells.

The ADCP moorings measure pressure at the depth of instruments (generally 1-1.5m from the seabed). Timeseries of bottom pressure were transformed into surface elevation by subtracting the deployment-averaged pressure (as an estimate of the local depth). In long and deep deployments this is a reasonable assumption, but errors will be introduced when taking this approach to short, shallow and coastal regions such as those inside the estuary. There, river and wind can sustain non-tidal elevations and bias the estimate of the depth. The over estimation of the along coast wind component (U component) will also produce significant biases in the bottom depth estimated this way due to coastal wind pill-up.

Table 3 Summary statistics of model-observation comparisons for all ADCP moorings covering years with AMM7 forcing (2017-2018) andAMM15 forcing (2019-2021). Data include estuarine stations and L4. Note that period 2019-2021 have more estuarine deployments that the period 2019-2021 have more estuarine deployments than 2017-2018.

Station	Variable	Year	Correlation	R^2	Bias	Root Mean Square	Mean Absolute Error
All	Surface elevation	2017-2018	0.97	0.83	0.07	0.57	0.45
All	Depth averaged current speed	2017-2018	0.72	0.76	0.03	0.11	0.08
All	U Depth averaged current	2017-2018	0.59	0.69	-0.00	0.10	0.07
All	V Depth averaged current	2017-2018	0.75	0.62	0.01	0.10	0.07
All	U surface current	2017-2018	0.64	0.67	0.00	0.11	0.08
All	V surface current	2017-2018	0.72	0.60	0.00	0.12	0.09
All	Bottom temperature	2017-2018	1.00	1.00	0.10	0.66	0.58
All	Surface elevation	2019-2021	0.90	0.69	0.06	0.79	0.55
All	Depth averaged current speed	2019-2021	0.61	0.48	0.03	0.16	0.12
All	U Depth averaged current	2019-2021	0.41	0.30	0.00	0.18	0.14
All	V Depth averaged current	2019-2021	0.75	0.24	0.01	0.10	0.06
All	U surface current	2019-2021	0.38	0.25	0.00	0.20	0.16
All	V surface current	2019-2021	0.53	0.17	0.01	0.13	0.08
All	Bottom temperature	2019-2021	0.98	1.00	0.30	0.54	0.42

Surface elevation during some of the deployments at L4 (Figure 4) illustrates the overall good correspondence (correlation coefficient of >0.9, r^2 >0.7, 3) and no obvious systematic bias with a maximum discrepancy of ~10% the observed tidal range. There is some variation with year (Figure 5) but no significant change between AMM7 and AMM15 periods.

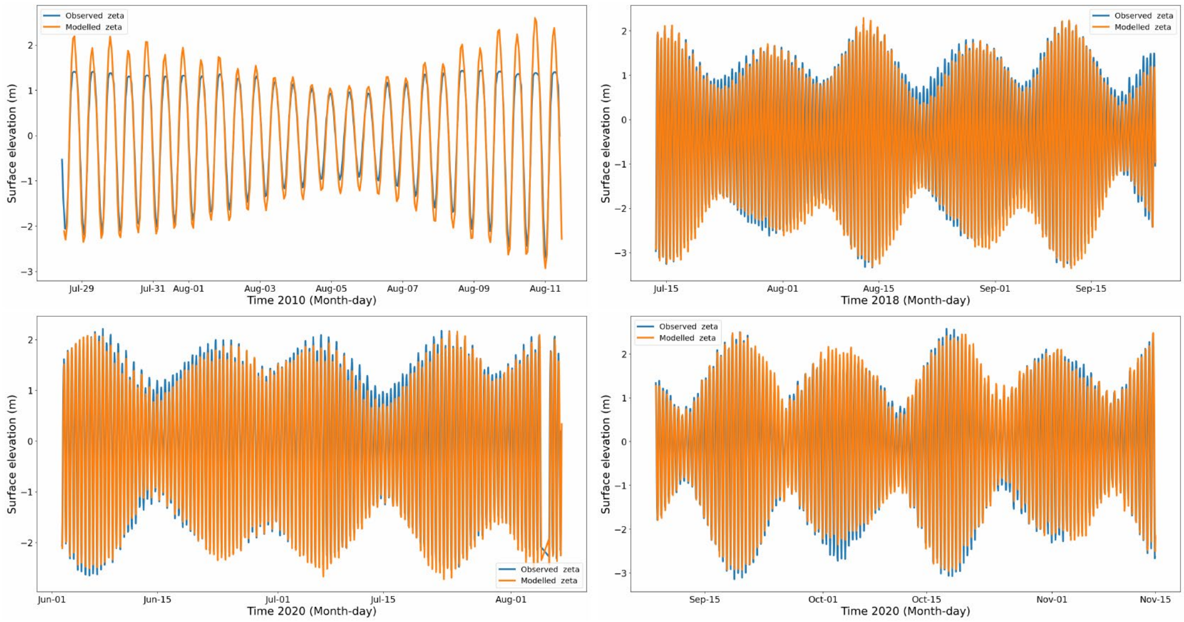

Figure 4 Time evolution of surface elevation for L4 deployments. Data represents 20 minute averages while model outputs are hourly.

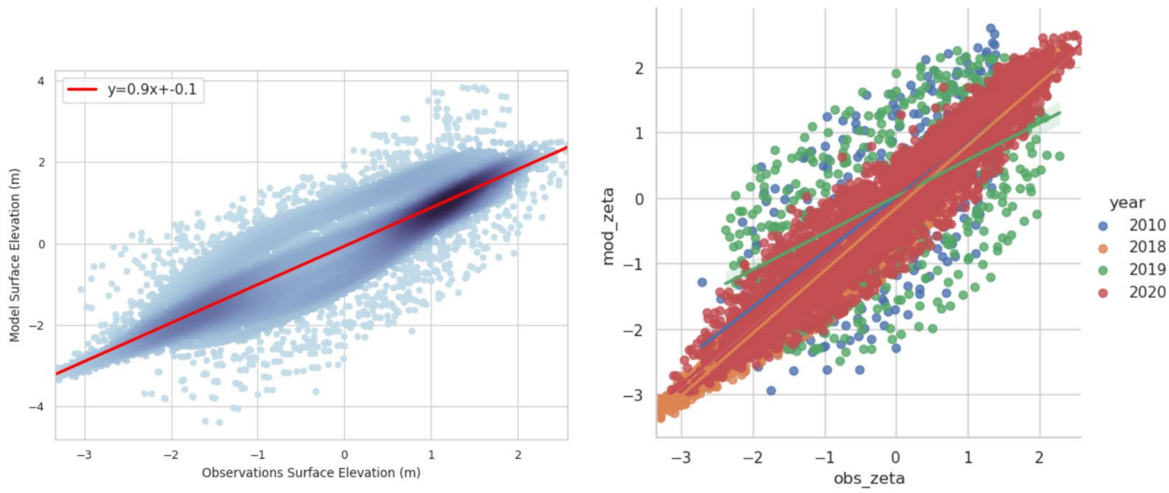

Figure 5Least square linear regression of nearest points for all years of data at L4. All data grouped (left) and regression lines and data points coloured by year (right).

The currents show larger variance and lower correlations than surface elevation as is generally the case in dynamic coastal areas. We obtained correlation coefficients that ranged 0.75-0.4 and r 2 >0.76-0.3. Overall, the model underestimates all currents evaluated (depth mean magnitude, components and surface components) at both the estuarine and coastal locations, but the fit to observations is generally better at the coastal L4 site than in the Plymouth Sound moorings. In this initial evaluation, there are indications that the model performance deteriorates during the AMM15 period (Figure 6) although the statistical significance has not been assessed. The data distribution of the depth mean current (Figure 7) suggests that the model underestimated the variance during the AMM7 period with respect to the observations while it overestimated during the AMM15 period but in both periods, it captured the inter-station differences.

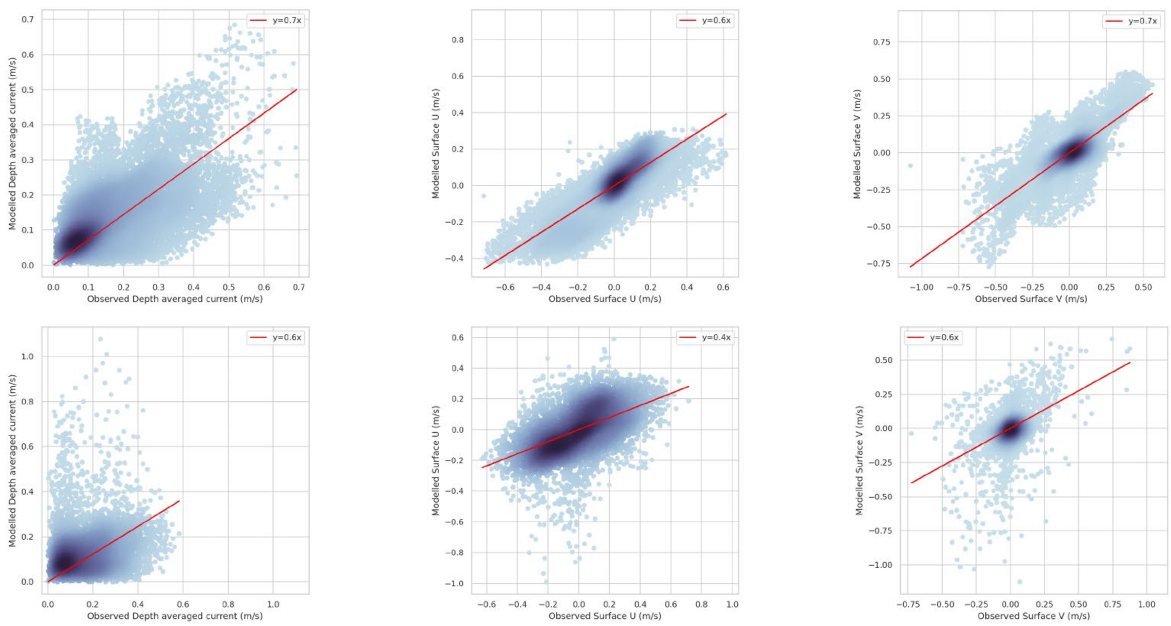

Figure 6 Least square linear regression of nearest points for all stations grouped by AMM7 (top) and AMM15 (bottom) periods for depth mean current magnitude and U and V surface current components.

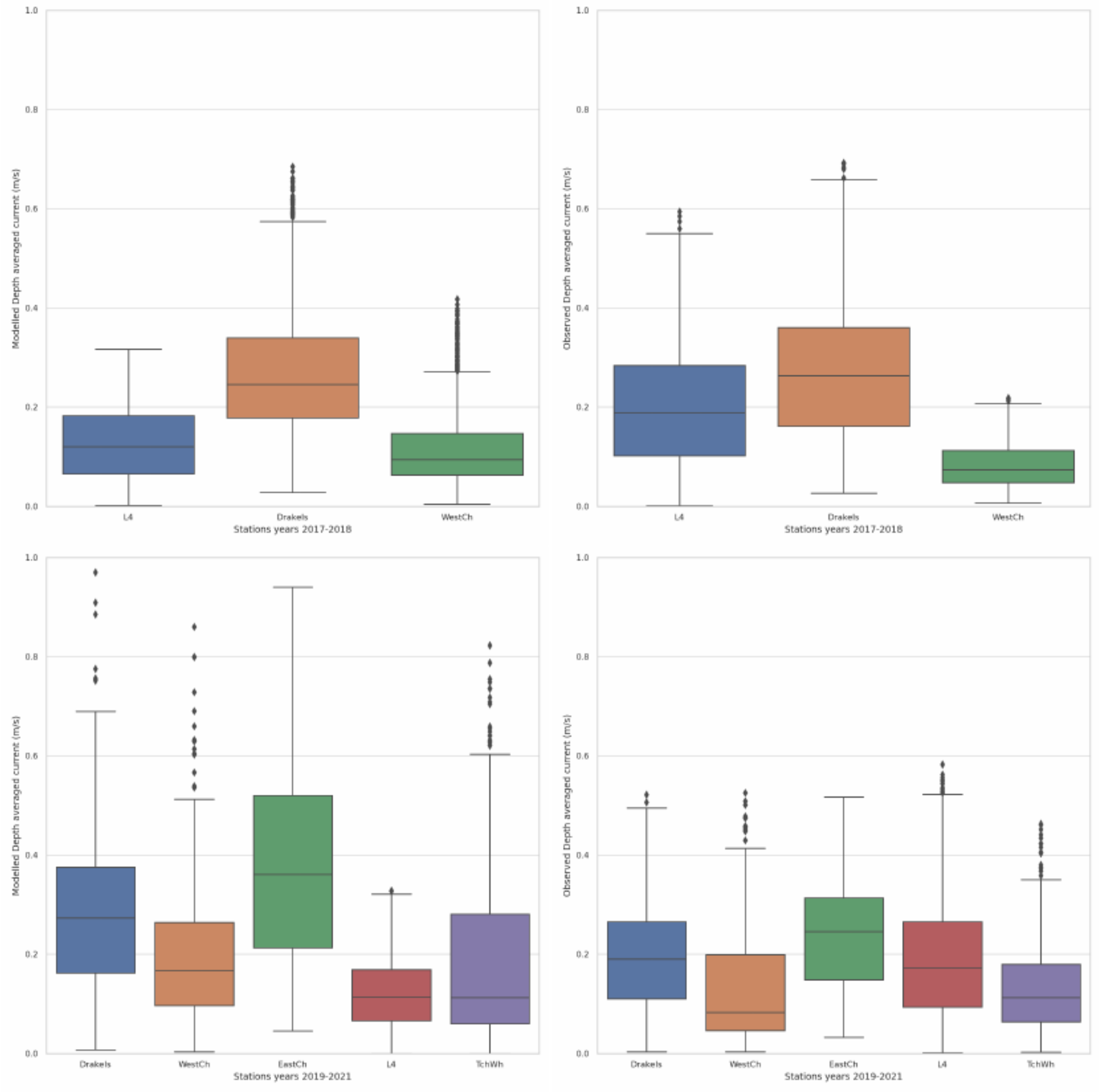

Figure 7 Box-whisker plots grouped by stations of the modelled (left) and observed (right) depth mean current during the AMM7 (top) and AMM15 (bottom) periods.

References:

Chen, C., H. Liu and R. C. Beardsley (2003). "An Unstructured Grid, Finite-Volume, Three-Dimensional, Primitive Equations Ocean Model: Application to Coastal Ocean and Estuaries." Journal of Atmospheric and Oceanic Technology **20**(1): 159-186.

Codiga, D. L. (2011). Unified Tidal Analysis and Prediction Using the UTide Matlab Functions. University of Rhode Island, Narragansett, RI, USA, Graduate School of Oceanography.

Egbert, G. D., A. F. Bennett and M. G. G. Foreman (1994). "TOPEX/POSEIDON tides estimated using a global inverse model." Journal of Geophysical Research **99**(C12): 24821-24852.

Egbert, G. D. and S. Y. Erofeeva (2002). "Efficient Inverse Modeling of Barotropic Ocean Tides." Journal of Atmospheric and Oceanic Technology **19**(2): 183-204.

Egbert, G. D., S. Y. Erofeeva and R. D. Ray (2010). "Assimilation of altimetry data for nonlinear shallow-water tides: Quarter-diurnal tides of the Northwest European Shelf." Continental Shelf Research **30**(6): 668-679.

Haney, R. L. (1991). "On the Pressure Gradient Force over Steep Topography in Sigma Coordinate Ocean Models." Journal of Physical Oceanography **21**(4): 610-619.

Legrand, S., E. Deleersnijder, E. Delhez and V. Legat (2007). "Unstructured, anisotropic mesh generation for the Northwestern European continental shelf, the continental slope and the neighbouring ocean." Continental Shelf Research **27**(9): 1344-1356.
Smagorinsky, J. (1963). "General Circulation experiments with the primitive equations I. The basic experiment." Monthly Weather Review **91**(3): 99-164.
Umlauf, L. and H. Burchard (2005). "Second-order turbulence closure models for geophysical boundary layers. A review of recent work." Continental Shelf Research **25**(7–8): 795-827.
Wessel, P. and W. H. F. Smith (1996). "A global, self-consistent, hierarchical, high-resolution shoreline database." Journal of Geophysical Research **101**(B4): 8741-8743.